Curve Monitoring for a Single-Crystal Ingot Growth Process

Liang Zhu[a], Chenxu Dai[b], Hongyue Sun[c],Wei Li[a], Ran Jin[c], Kaibo Wang[b]

[a]: The State Key Lab of Fluid Power Transmission and Control, Zhejiang University, Hang Zhou, 310027, China

[b]: Department of Industrial Engineering, Tsinghua University, Beijing, 100084, China

[c]: Grado Department of Industrial and System Engineering, Virginia Tech., VA 24061, USA

Abstract

In conventional statistical process control, a conforming process is usually assumed to be stable with a constant mean value. However, dynamic data streams of variables over time are widely encountered in many complex manufacturing processes. In this paper, we study the ingot growth process, which exhibits a time-varying mean and variance even if the process is in-control. We propose different charting schemes for the statistical monitoring of the process. The performance of the new charts are compared via simulation. Implementation of the newly proposed chart to the real data shows that the chart is effective in detecting process failures in the growing curves.

Key words: control chart, manufacturing process, quality control, statistical process control

1. Introduction

Statistical process control (SPC) has been widely used in practice to investigate industrial processes and improve quality (Woodall, 2000). One of the major tools, a control chart, is usually set up to monitor key process variables or quality characteristics, and trigger alarms when assignable-cause variation is detected. By removing such variation sources, the total variability of the process is expected to be reduced.

A control chart can be viewed as a graphical tool for quality control. When a sample becomes available, a charting statistic is calculated based on the sample, and a point that reflects the charting statistic is plotted on the chart. If the point falls outside the control limits, the process is concluded to be out-of-control. Then the procedure of searching for root causes shall be carried out.

In control chart implementation, one common assumption is that the distribution of the monitoring statistics from an in-control process remains unchanged, such as the mean and variance are assumed to be constant for a conforming process as shown in Figure 1. For this Shewhart control chart, the control limits are calculated based on the unchanged mean and variance from the in-control process. If the observed sample falls beyond the control limits, an out-of-control signal is triggered.

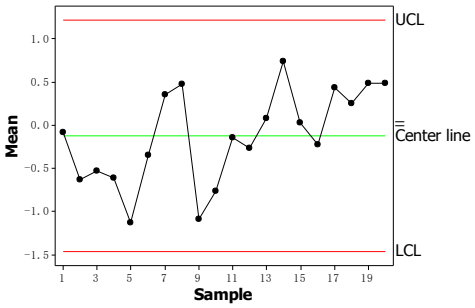

Figure 1. A typical control chart with constant mean and variance

It has been widely studied when the process exhibits dynamic shift patterns. For example, in an inertia process, when a shift occurs, the resulting shift pattern follows a particular trend (Wang and Tsung, 2008). In a feedback-controlled process, a sudden shift in the process may lead to oscillated (Wang and Tsung, 2007) or cyclical (Tsung and Tsui, 2003) signals. However, in these methods, the mean of the process is assumed to be a constant.

There are cases in which the mean of the process is unstable. Spitzlsperger *et al.* (2005) is one of the few methods in the literature that has noticed this issue. The authors studied an etching process. Due to the accumulating effect, some parameters drift slowly in the normal operational runs and are reset when chamber cleaning happens. The variation of the parameters also changes over time. Jin and Liu (2012) also proposed a regression tree based method to cluster and estimate multiple baseline distributions for an in-control process, and develop control chart for each cluster. However, the existing work failed to consider the scenarios that the normal mean and variance are both changing with time when the process is in-control.

In this paper, we study an ingot growth process that is widely used in semiconductor manufacturing. We focus on the power consumption of the heater, which is one key process variable to affect ingot quality. The ingot growth process is a very complicated chemical-physical process. Figure 2 shows a photo of the equipment. The lower part of the equipment contains a quartz crucible, which is protected by insulation layers and used to melt raw silicon material. The upper part is the pulling chamber. In production, the raw silicon material is firstly melt; a crystal seed attached to a pulling thread touches the liquid surface and initiates the growth of the single-crystal silicon ingot. With the thread pulling up slowly, the single-crystal ingot grows. In the whole process, the power is a critical parameter that may determine the success or failure of the growth process.

Figure 2 The single-crystal ingot growing furnace

Figure 3 shows the power over time from a conforming growth process. At the beginning of the growth process, the power increases sharply, then decreases and oscillates after reaching an initial peak point. After several hours, the process becomes stable, and the power varies slightly around a mean value. In the final stage of the process, the power increases slowly again until the process finishes. The sharp increase is because more power is required to melt the silicon crystal at the beginning stage of the process. Then the required heat gradually decreases as the ingot grows.

In the crystal growth process, the thermal gradient in the furnace is critical to the successful formation of the single crystal and the quality of ingots. The thermal gradient is jointly determined by the power, the heat preservation of the insulation layer, and the positions of the ingot and the crucible. As the ingot grows longer, the position of the ingot and the crucible is also changing. The furnace control system will automatically adjust the power to compensation the heat loss, and maintain the thermal gradient in the furnace. Therefore, this dynamically changing curve is considered normal in the process.

When some unexpected changes occur, it is possible that the process become nonconforming. Figure 4 shows an abnormal power curve from another furnace. Although the early and middle stage of the power curve shows a similar pattern as the one in Figure 3, the means and variances of these two curves differ. This is mainly because the insulation layers in these two furnaces have different heat preservation effects due to different reliability conditions of the insulation layers. Moreover, the power curve in Figure 4 has strong oscillation near the end of the process. The ingot becomes failed at this time. The square mark shows the time point at which the process failure was identified by the operator, where the actual failure time is before this point.

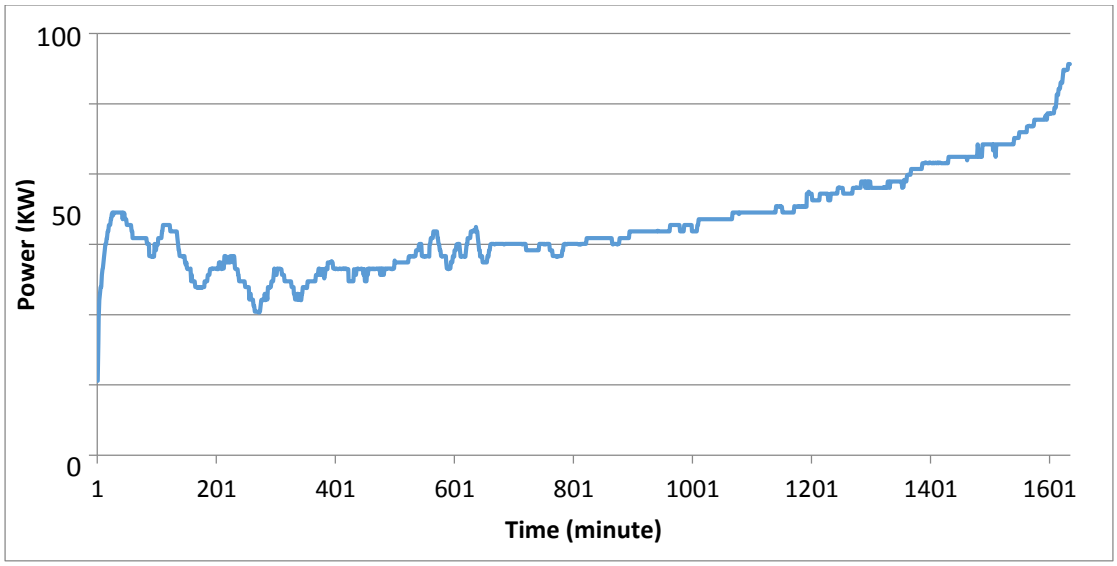

Figure 3 Time series plot of power in a normal run

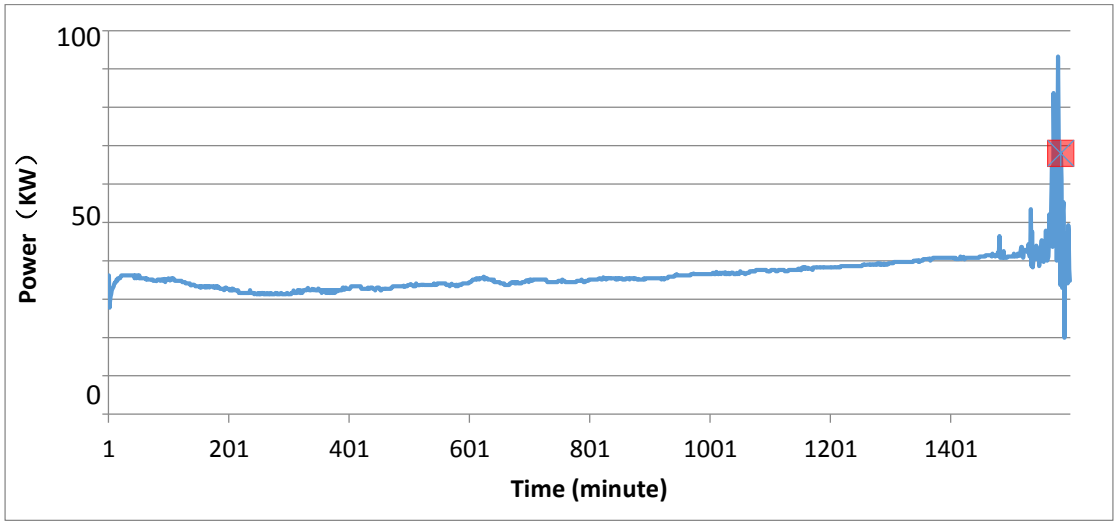

Figure 4 Time series plot of power in an abnormal run

Beyond the crystal growth process, such growing curves are widely encountered. A growing curve is a profile that extends/grows over time. It reflects the change of a quantitative variable in the time domain. For example, the wire slicing speed is slow at the beginning of the wafer slicing process, and becomes faster as the contact span increases. Different equipment will use different speed curves as the equipment maintenance conditions are not identical. Such growing curves share some common features: a) the in-control mean patterns shows a dynamic trend, i.e., a single baseline distribution is not adequate for the monitoring statistics, or the dynamic trend cannot be adequate modeled by a baseline model such as linear regression models or polynomial functions; b) the dynamic trend differs for different batches or equipment. This raises the challenge to control chart design in term of determining the in-control parameters, the center line

and the control limits. Therefore, in this work, we propose new control charts to address these challenges.

The rest part of the paper is organized as follows. In Section 2, we first review relevant works on control charts. In Section 3, we propose different charting schemes to monitor such dynamic growing curves. The performance of the new charts is studied in Section 4 by both extensive simulation and a real data set. Finally, conclusions and topics for future research are suggested in Section 5.

2. Review of related charting techniques

There is a rich body of literature developed for control charts with a constant mean, such as the Shewhart (1926) chart, the cumulative sum (CUSUM) chart, and the exponentially moving average (EWMA) chart.

The EWMA chart is one of the most import charts for monitoring processes with small shifts. The common form of the EWMA chart is given by

$$z_t = \lambda x_t + (1-\lambda) z_{t-1}$$

where x_t is the observation; λ is a smoothing parameter that determines the weight assigned to historical observations, $0<\lambda<1$. A small value of λ can help quickly detect small changes in the mean shift and a larger value is helpful for quickly detecting the occurrence of large shifts.

It is difficult for a single EWMA control chart to get a "minimum ARL value for both small and large mean shifts (Crowder, 1987; Lucas and Saccucci, 1990). Yashchin (1987) discussed the inertia problem of the EWMA scheme. When the charting statistic is close to the upper control limit, a sudden change in the opposite direction creates inconsistency in the process. Therefore, the EWMA control chart with smaller value of λ should overcome the inertia to react with sudden shift changes (Woodall and Maragah, 1990). The inertia problem can also be solved by adding Shewhart limits to an EWMA control scheme. When the EWMA statistic falls outside of the Shewhart limits, or the current observation is out of the Shewhart limits, an out-of-control signal is generated (Lucas and Saccucci, 1990; Albin *et al.* 1997).

The EWMA control scheme was further improved by Capizzi and Masarotto (2003), in which a new chart named the adaptive exponentially weighted moving average (AEWMA) control scheme was proposed. The AEWMA chart combines the EWMA and Shewhart in a smoother way to reduce the inertia. In contrast to the method introduce by Lucas and Saccucci (1990), the AEWMA chart uses an adaptive smoothing parameter, which changes with observations. Therefore, the AEWMA chart is better for detecting shifts with an unknown magnitude of shifts. However, the AEWMA chart also assumes that the process mean is a constant. In this work, we will modify the AEWMA chart and borrow the algorithm for process updating.

The curve shown in Figure 3 and Figure 4 are typical functional profiles. In the literature, extensive research has been seen for profile monitoring. A comprehensive review is given in Woodall (2007). In profile monitoring, it is normally assumed that n ($n > 1$) values of a response variable are measured along with the corresponding values of one or more explanatory variables. Woodall *et al.* (2004) described the monitoring in two phases and discussed issues regarding profile monitoring. Profile monitoring has normally been shown as a simple linear regression model. Chang and Gan (2006) proposed Shewhart control charts for monitoring the slopes of the relationships between two or more measurement processes in order to assure their accuracy. Zhu and Lin (2009) considered using slope in profile monitoring in Phase I and Phase II. Noorossana (2004a) proposed a new method for monitoring simple linear regression profiles based on the multivariate control chart method of Healy (1987). A self-starting method was proposed Zou *et al.* (2007) in which they avoided using distinction between the two phases of control. Mahmoud and Woodall (2004) and Zou *et al.* (2006) considered change-point methods for detecting changes in the parameters of a simple linear regression model. These authors considered Phase I and Phase II applications, respectively. Gupta *et al.* (2006) used a different approach of profile monitoring in which the estimated regression parameters is more effective in terms of the run length performances.

Although the curve considered in this paper is a profile, the requirement for monitoring is quite different from the conventional scenarios. In the profile monitoring literature, each profile is treated as one sample; when calculating the charting statistic, the whole profile is known. In our work, the curve is a *growing* curve, the length of which extends with time; decisions must be made each time a new point is obtained from the profile. Thus, the conventional profile monitoring method cannot be used to this problem directly.

3. Control charts for growing curves

In this paper, we will monitor potential mean and/or variance shifts of the growing power curves. As aforementioned, the power curve to be monitored has two distinct features. First, the curve shows a dynamic trend. Thus, the mean and variance of the curve are not constant with time goes by. Second, the curve exhibits different patterns for different equipment. Therefore, a learning algorithm is needed to track the in-control parameter of each run in different equipment. In the following, we proposed different ways to tackle these problems, and study their performance via simulations.

3.1 An adaptive EWMA chart

Since the power curve exhibits a slow changing trend, a natural choice of the leaning algorithm would be the EWMA method. However, as the sample curve in Figure 3 shows, the power varies quickly in the initial stage, the EWMA algorithm shall prefer a large smoothing parameter so that the quick changing trend can be captured; nevertheless, in the later stage, the curve only changes slowly, and a small smoothing parameter shall be preferred. Therefore, in the first proposed scheme, we use the following adaptive EWMA algorithm, which was first suggested by Capizzi and Masarotto (2003), to track the mean of the dynamic process

$$\mu_t = \left(1 - w\left(e_t\right)\right)\mu_{t-1} + w\left(e_t\right)x_t \tag{1}$$

where $w\left(e_t\right) = \phi(e_t)/e_t$ is the weighting function; and $e_t = x_t - \mu_{t-1}$ is the estimation error. As suggested by Capizzi and Masarotto (2003), the following weighting function has been proven effective and is therefore adopted in this work:

$$\phi(e_t) = \begin{cases} e_t + (1-\lambda)k & \text{if } e_t < -k \\ \lambda e_t & \text{if } |e_t| < k \\ e_t - (1-\lambda)k & \text{if } e_t > k \end{cases}$$

However, in the adaptive EMWM procedure proposed by Capizzi and Masarotto (2003), the authors assumed that the variability of the process remains unchanged, and thus only mean changes are monitored. In our target process, since the variance of the process also changes over time, we need to update the standard deviation of the variable. Similar to the EWMA method for mean update, here we borrow the method proposed by Macgregor and Harris (1993) and update the estimate of process standard deviation as follows:

$$\hat{\sigma}_t = \sqrt{(1-\gamma)\hat{\sigma}_{t-1}^2 \times + \gamma\left(x_t - \mu_{t-1}\right)^2} \tag{2}$$

where γ is a smoothing parameter. The magnitude of γ decides the speed of parameter update.

Finally, the control chart for monitoring the dynamic growing curve is:

$$\begin{cases} UCL = \mu_t + 3\hat{\sigma}_t \\ CL = \mu_t \\ LCL = \mu_t - 3\hat{\sigma}_t \end{cases}$$

where the center line, μ_t, is updated using the adaptive EWMA equation in Equation (1). Whenever a new point becomes available and the chart is in-control, we update the center line; if the point becomes out-of-control, according to Spitzlsperger *et al.* (2005), the center line remains unchanged. As this chart is essentially derived from the adaptive EWMA chart, we name this chart the *AEWMA* chart. This chart is equivalent is to monitor the adjusted residual $e_t = x_t - \mu_{t-1}$, and triggers and alarm when the residual is extremely large or small. Different from the conventional $\bar{x}$ or individual chart, the control limits of the proposed chart changes with time, as $\hat{\sigma}_t$ is updated continuously each time a new observation becomes available.

In this proposed algorithm, the parameters λ decides the amount of weight assigned to new observations, and k is the threshold for estimation errors. If the estimation error e_t is large, $w(e_t)$ shall approach one, and the updated values is essential the new observation, which is

similar to a Shewhard control chart; if the estimation error is small, $w(e_t)$ approaches λ, the mean is then updated following the conventional EWMA equation. Capizzi and Masarotto (2003) noted that the former part is beneficial to quick changes, and the later part is beneficial to small changes. Therefore, the adaptive EWMA method combines the advantages of the Shewhart-type chart and the EWMA chart, and it is expected to perform well in tracking the dynamic mean of the growth curve.

It should be noted that the choice of λ is critical. If $|e_t| < k$, the effective smoothing parameter is λ; if $|e_t| > k$, the effective smoothing parameter is larger than λ. Thus, the parameter λ and k should not be too large.

3.2 An joint EWMA chart for the growing curve

Reynolds and Stoumbos (2006) studied charts that can jointly monitor the mean and variance of a process. The joint scheme was not original designed for the growing curve that we encountered in this paper. As the EWMA procedure can be adapted to track slow changing trends, we modify the joint EWMA scheme to fit with the growth process variables.

The scheme estimates process mean using the following equation

$$E_t^{\,M} = \left(1-\lambda^M\right) E_{t-1}^{\,M} + \lambda^M X_t$$

and uses the following as control limits for the mean:

$$E_t^{\,M} \pm h^M \sigma_t \sqrt{\lambda^M / \left(2-\lambda^M\right)}$$

Different from Reynolds and Stoumbos (2006) which assumes a constant variance estimate in the mean chart, here we calculate $\widehat{\sigma_t}$ using Equation (2) to account for the varying standard deviations of the process. $E_t^{\,M}$ is the statistic for mean EWMA chart, λ^M is a tuning parameter, h^M determines control limits and is selected based on a pre-specified false alarm rate or ARL, and $E_0^{\,M} = X_1$.

The joint charting scheme has another EWMA chart for monitoring changes in the process variance, which takes the following form

$$E_t^{\,V} = (1-\lambda^v)\max\{E_{t-1}^{\,V}, \widehat{\sigma_t}^{\,2}\} + \lambda^v\left(X_t - E_{t-1}^{\,M}\right)^2$$

with control limits

$$E_k^{\,V} \pm h^v \widehat{\sigma_t}^{\,2} \sqrt{2\lambda^v/(2-\lambda^v)}$$

where E_t^V is the statistic for variance EWMA chart and $E_0^V = \hat{\sigma}_t^2$, other parameters has similar meaning as those in the mean chart.

As this scheme uses two EWMA charts and is applied to the growing curve, we name this chart the joint EWMA for curves (*J-EWMA-Curve*) chart; its performance will be studied and compared with other charts in a later section.

3.3 An joint EWMA chart for residuals

In the AEWMA scheme, the process mean is updated using Equation (1), and the residual series, $e_t = x_t - \mu_t$, are derived. Once the dynamic mean pattern is removed, it becomes feasible to monitor the residual series assuming the process is stable. Therefore, we also propose to monitor the residual using the above joint EWMA scheme, that is, apply the joint EWMA scheme to the residual sequence. As the chart is applied to the residual sequence, we name this scheme the joint EWMA for residuals (*J-EWMA-Residual*) chart and study its performance in the next section.

3.4 Profile monitoring techniques

Yu *et al.* (2012) proposed a method for Phase I profile outlier detection. When a curve of certain length is given, the method can be used to compare a new curve with a batch of existing ones. That is, for this method to work, the complete curve must be given. The detailed method is referred to the original work of Yu *et al.* (2012).

As the curve we encountered is a growing curve, the method proposed by Yu *et al.* (2012) need to be modified before it could be applied. Since the detection algorithm relies on a mean curve, and the curves in the simulation setting differ from each other, we first fit an autoregressive (AR) time-series model to each curve. The residual sequence, where the dynamic mean in the original variable is removed, will be monitored using the method proposed by Yu *et al.* (2012). The detailed simulation procedures used in this work are summarized as follows:

1) We generate a set of curves as Phase I data, fit an AR(1) model to each curve, then calculate the residuals based on the time series model. The residual curve is treated as the in-control path of the process. To mimic the real-time growing behavior of the process while considering the requirement for a complete curve for the method to work, we wait until 31 points on each curve is collected to fit the AR(1) model and monitoring its status. After the 31st step, the AR(1) model is updated when new observations becomes available; the residual sequence is also updated with the AR model. Due to computation limitations, the update is carried out every 3 steps.
2) For a new on-line curve, we calculate the residual sequence in the same way as above; then based on the residual sequences of the new online curve and in-control baseline curves, we conduct principal components analysis following the method in Yu *et al.* (2012).

3) Based on the principal component (PC) score obtained in Step 2, we calculate the testing statistic for the online curve, and compare the testing statistic with a pre-defined threshold value to check the status of the process.

As this chart is derived from a profile testing algorithm applied to the AR residual sequence, we name this method the *Profile-Residual chart*. In the following, we study the performance of the different schemes and identify their respective advantageous and disadvantageous.

4. Performance study

To study the performance of the proposed methods, we first use Monte-Carlo simulation to investigate the performance of the different charting schemes. Then, for demonstration purpose, we apply one chart to a real data set to demonstrate its effectiveness in real applications.

4.1 Settings for process simulation

To mimic the dynamics of the ingot growth process, we construct the following two-stage model, which has a similar trend as the real process

$$\mathrm{y}_t = \begin{cases} K + a\sin\left(\dfrac{t}{\omega}\right) + \varepsilon_{1t}, \varepsilon_{1t} \sim N(0, \sigma_t), if\ 0 < t \le T \\ y_T + b(t-T) + \varepsilon_{2t}, \varepsilon_{2t} \sim N(\mu_2, \sigma_t), if\ T < t < T + 30/b \end{cases}$$

The first stage of the function changes as a sinusoidal wave, and the second stage follows an increasing linear trend. The in-control settings shown in Table 1 are used to generate simulated samples. Each simulated process runs for 79 steps; correspondingly, each growing curve to be monitored contains 79 readings.

For comparison purpose, we assume that when the process is out-of-control, the process follows

$$\mathrm{y}_t = \begin{cases} K + a\sin\left(\dfrac{t}{\omega}\right) + \varepsilon_{1t}, \varepsilon_{1t} \sim N(0, \sigma_t), if\ 0 < t \le T \\ y_T + b'(t-T) + \varepsilon_{2t} + \delta, \varepsilon_{2t} \sim N(\mu_2, \sigma_t), if\ T < t < T + 30/b \end{cases}$$

Three failure modes are studied, including variance shift, mean shift, and mean drift. For each failure mode, different shift magnitude is studied. The detailed settings of the shift magnitude are shown in Table 2. Figure 5 shows samples from the in-control process and different out-of-control modes. When generating out-of-control samples, the variance shift, mean shift, and mean drift are added to the process at Step 45, 45 and 55, respectively.

Table 1. In-control settings used in numerical simulations

Parameters	Explanation of the parameter	Value used in simulation	Notes
K	Position of the curve	0	K does not affect the charting performance
a	Amplitude of sinusoidal function	5~10	a random value from uniform [5, 10] distribution
b	Slope of the linear function	0.75	Same reason as above
ε_t	Variation of the profile	$\sigma_t = 1.5e^{-0.01t}$	Increase by 0.5 units of $e^{-0.01t}$ at each step
ω	Length in x-axis of sinusoidal function	6	
T	Length of stage 1	$2\pi\omega$	
μ_2	Mean of the disturbance in stage 2	0	

Table 2. Out-of-control settings for numerical simulations

	Severity of failure		
Variation shift	$\sigma_{t>T} = 2e^{-0.01t}$	$\sigma_{t>T} = 4e^{-0.01t}$	$\sigma_{t>T} = 6e^{-0.01t}$
Mean shift	$\delta = 5$	$\delta = 8$	$\delta = 11$
Mean drift	$b' = b + 0.7$	$b' = b + 0.9$	$b' = b + 1.1$

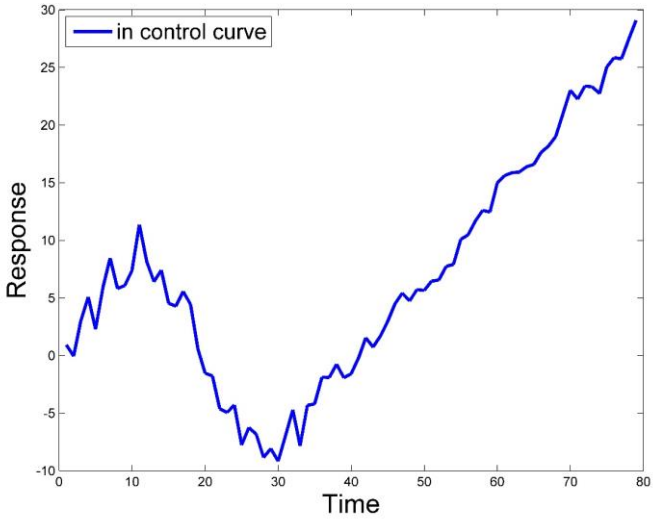
in control curve
Response
Time

(a)

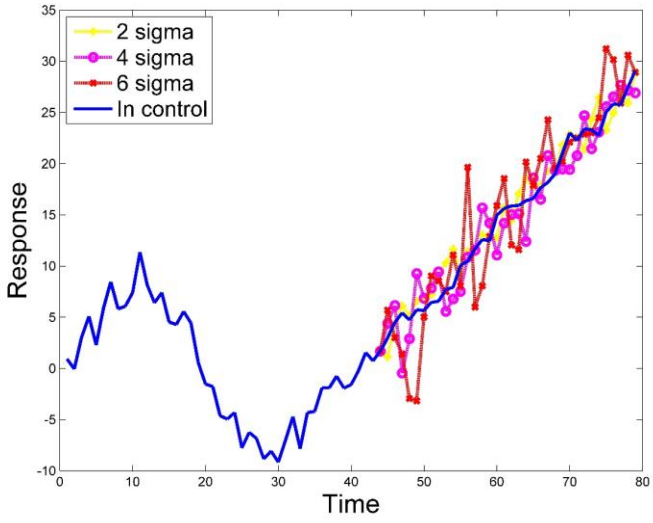
2 sigma
4 sigma
6 sigma
In control
Response
Time

(b)

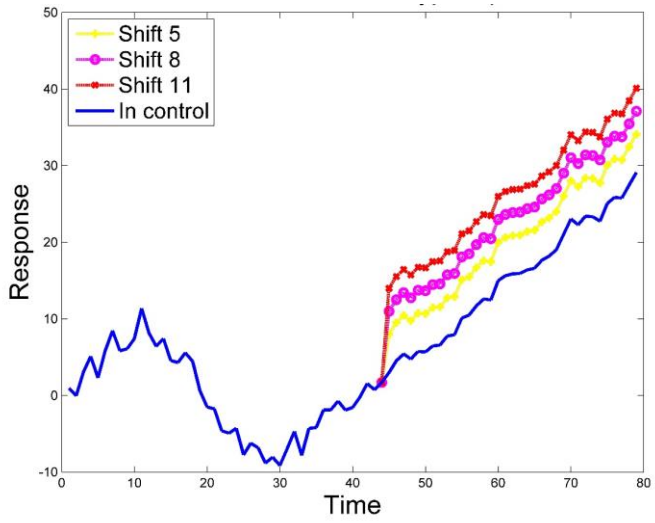

(c)

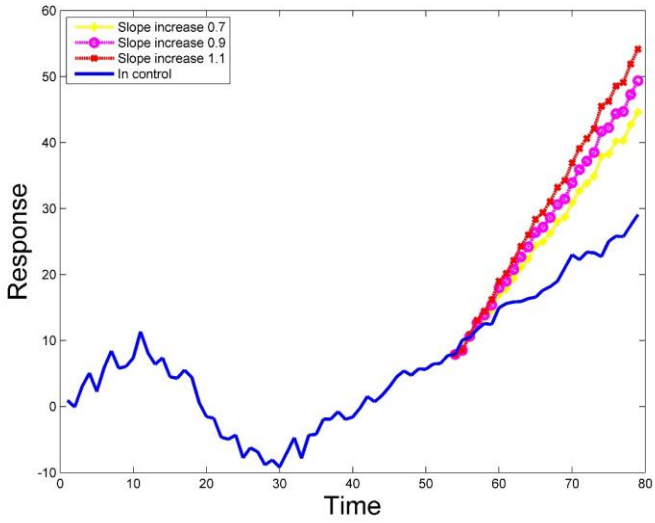

(d)

Figure 5. Sample in-control and out-of-control curves. (a) in-control, (b) with variation shift, (c) with mean shift and (d) with mean drift

4.2 Settings for competing control charts

To study the performance of the charts, 5000 in-control and 5000 output-of-control curves for each failure mode are generated and monitored by the charts. For a fair comparison, the control limits of all charts are adjusted so that they have an equal false alarm rate of 100 out of 5000 when the process is in-control. More specifically, the AEWMA chart uses $\lambda = 0.4, \gamma = 0.01, k = 1$, the J-EWMA-Profile chart uses $\lambda^M = \lambda^v = 0.15$, $\gamma = 0.02$, $h^M = 2.5$ and $h^v = 5.1$, the J-

EWMA-Residual chart uses $\lambda^M = \lambda^v = 0.1$, $h^M = 4.6$ and $h^v = 8.6$, and the Profile-AR uses the threshold value $l_{N,d}(\alpha) = 51.975$.

For the different out-of-control scenarios, two indicators are presented. The first is the number of alarms received. This indicator represents the number of curves that are identified as out-of-control from the total 5000 out-of-control curves. If the curve is ever reported out-of-control, one alarm is recorded (and the chart stops so that each curve can trigger one alarm at most). So the maximum value for this indicator is 5000 (which means the chart successfully identified all out-of-control curves). The second indicator is the average run length (ARL), which is defined as the average time to signal of all the profiles (if the curve never signals, the total length is treated as its time to signal). Since the curve is growing with time, if the curve signals, the exact time the alarm is triggered is also important. We hope that the alarm occurs after the process shift and stay close to the change-point. If the alarm is triggered before the change-point of the process, the alarm is treated as a false alarm. As the change-point of the simulated processes is fixed, the number of false alarms does not vary with the shift magnitude. The simulation results are shown in Table 3.

Table 3. Performance comparison

Shift pattern	Shift size	AEWMA (# of alarms / ARL)	J-EWMA-Profile (# of alarms / ARL)	J-EWMA-Residual (# of alarms / ARL)	Profile-Residual (# of alarms / ARL)
Variation shift	$\sigma_{t>T} = 2e^{-0.01t}$	109/77.8	100/77.8	697/76.3	**734/77.5**
	$\sigma_{t>T} = 4e^{-0.01t}$	2294/66.3	100/77.2	**4996/51.4**	4946/58.9
	$\sigma_{t>T} = 6e^{-0.01t}$	4652/51.8	100/72.2	**5000/47.7**	**5000/52.6**
Mean shift	δ =5	**1898/65.6**	408/75.8	1008/71.7	436/77.9
	δ =8	**4868/45.4**	2773/59.7	4668/46.7	1796/73.1
	δ =11	**5000/44.5**	4813/45.8	4998/44.5	4101/59.7
Mean drift	b'=b+0.7	100/77.8	100/77.8	**245/77.8**	49/78.9
	b'=b+0.9	100/77.8	100/77.8	**5000/73.4**	63/78.9
	b'=b+1.1	100/77.8	100/77.8	**5000/69.7**	79/78.8

4.3 Simulation results analysis

Table 3 shows the number of alarms and ARL of the charts under different shift scenarios. For each shift scenario, the chart that gives the best performance (with the largest number of out-of-control alarms and the shortest ARL) is highlighted. It is learned from Table 3 that:

1) The AEWMA chart is insensitive to mean drift, but is sensitive to mean shifts. This happens since the slow drift may lead the adaptive EWMA procedure to a wrong directly, while a sudden shift is more prominent and cannot be eliminated by the EWMA procedure;

2) The J-EWMA-Residual is effective for all types of changes, and performance the best for mean drift and variance shift with moderate and large magnitude, while the J-EWMA-Profile chart is in-general inferior.
3) The Profile-Residual chart is good at detecting variation and mean shift, but is rather slow in detecting mean drift in the process.

Overall, the AEWMA chart is the best for detecting sudden mean shift, while the J-EWMA-Residual chart seems to perform well in general. In practice, the choice of the control charts heavily depends on the shift modes that one intends to detect. The above findings provide useful guidelines for the practitioners to select charts that best suits their individual applications.

4.4 Application to a real example

In this section, we applied the proposed charts to the ingot growth process. All the aforementioned charts could be implemented. While for demonstration purposes, here we only show how to apply the AEWMA chart to the real process.

Based on our analysis of the effects of the parameters, the following combinations give overall good charting performance: λ =0.4, γ =0.002, k =0.05. These settings are used to test all real samples. The total length of each curve is more than 1700 steps. Since the initial stage of the process increases quickly, the first 50 steps is used to warm-up the control chart. So, no alarm is released in the first 50 steps in all charts.

Figure 6 shows the control chart for the power curve of a normal ingot. It can be seen that with the process goes on, the power curve (the curve in the middle) changes dynamically, while the control limits also vary with the power curve, which shows the adaptability of the control chart to the system dynamics. In addition, the interval between the two control limits is shrinking when time moves; this shows that the variability of the process is decreasing. This is consistent with the real situation since the curve becomes smoother in the later stage. Figure 7 shows the estimation error of the process, i.e., $e_t = x_t - \mu_{t-1}$. It is clear that the error gives rather random pattern, and the mean trend has been successfully captured by the adaptive EWMA algorithm.

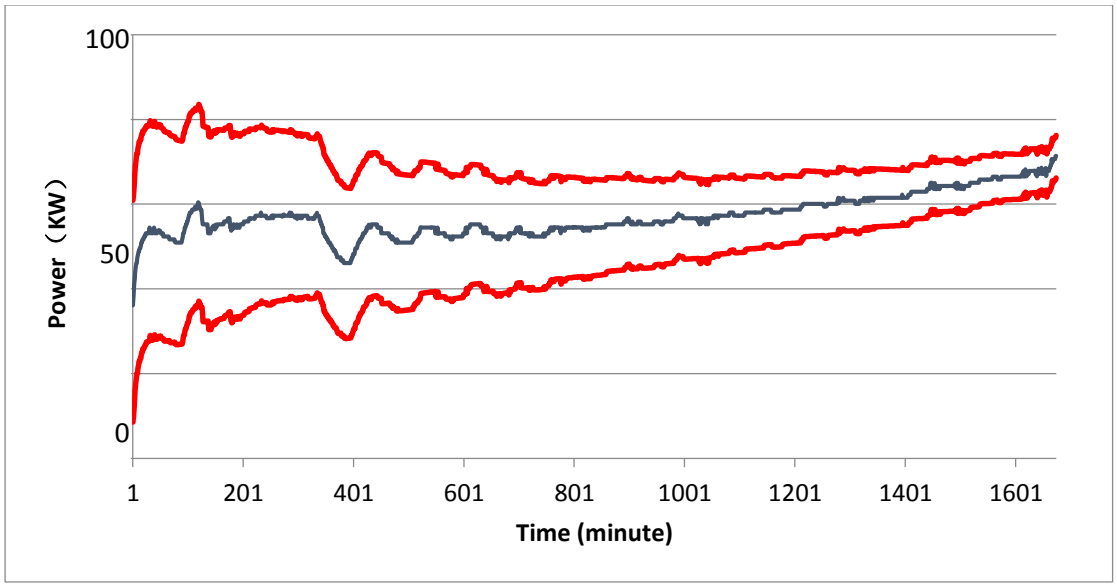

Figure 6. Control chart for the power curve of a normal ingot

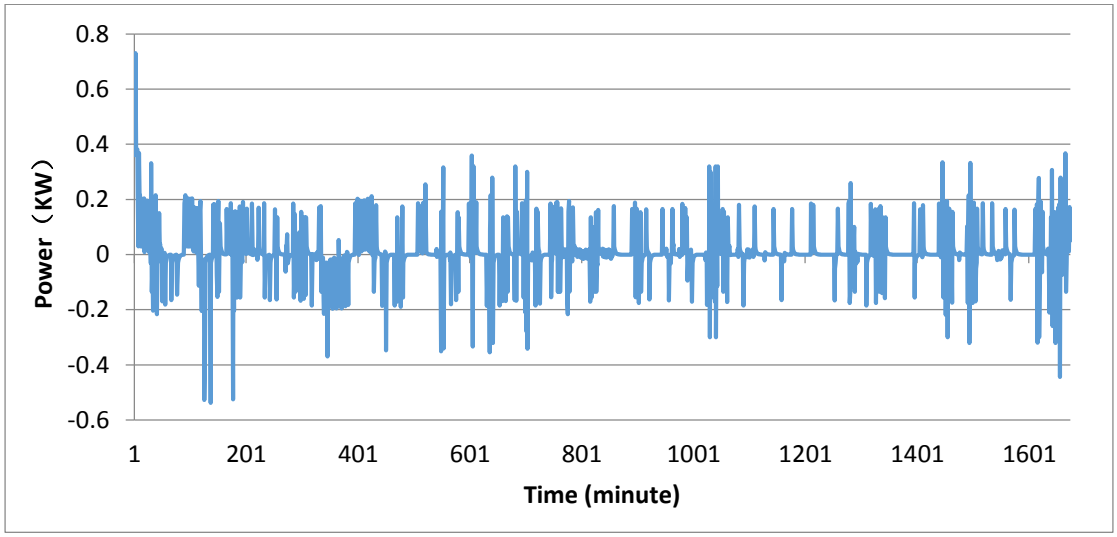

Figure 7. Prediction error of a normal ingot

Figure 8 shows the control chart for an abnormal ingot. The growth process is known to be failed from engineering knowledge. Figure 8 shows similar dynamic control limits as those in Figure 6. However, in the final stage, the power curve shows strong oscillation and the shift magnitude goes beyond the control limits. Further investigation shows that the diameter of the ingot becomes abnormal. Therefore, the new chart can successfully capture the failure. Compared to the failure discovered by the operator shown in Figure 4, the out-of-control signal is released nearly 90 minutes earlier by the proposed chart. Figure 9 shows the prediction error of the power curve, which shows random noise in the early stage and strong out-of-control signals in the later

stage. This further confirms the ability of the new chart in tracking process dynamics and detecting abnormal failure signals.

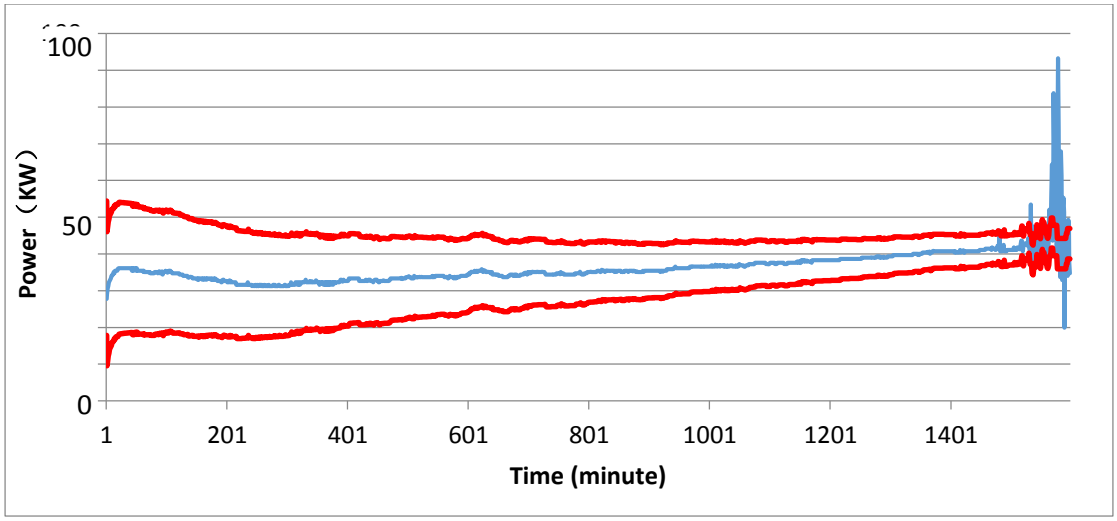

Figure 8. Control chart for the power curve of an abnormal ingot

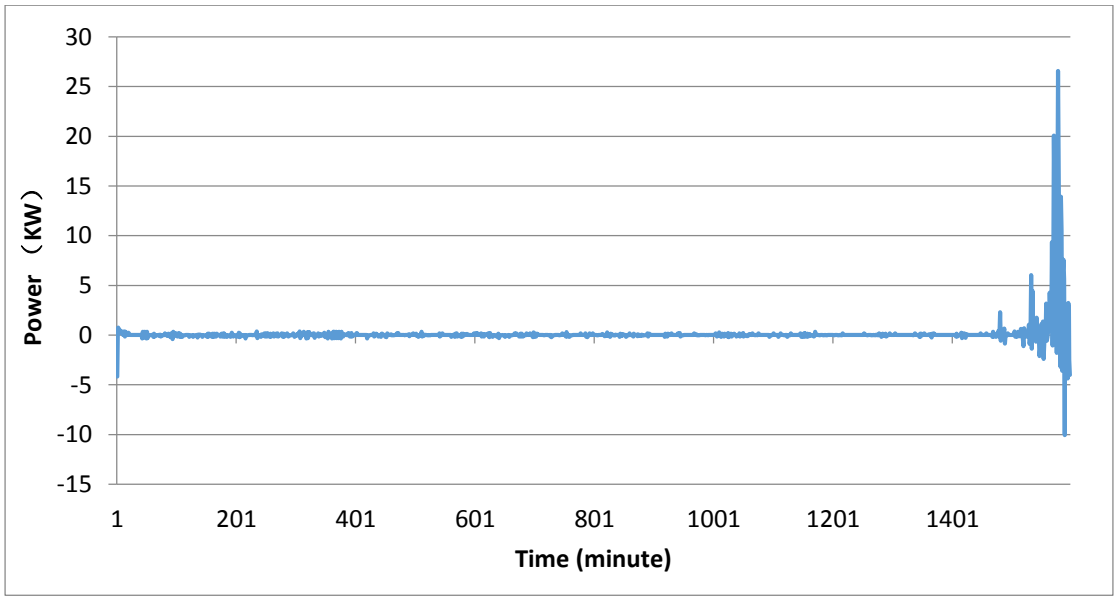

Figure 9. Prediction error of an abnormal ingot

5. Conclusions

Traditional control charts usually assume that the monitoring statistics follows an unchanged distribution when the process is in-control. However, in some engineering processes, strong dynamics are identified and unstable process means and variances are observed. In such cases, most conventional control charts cannot be applied directly.

In this work, we propose several new charting schemes for such dynamic processes. Simulation studies reveal that the AEWMA chart is sensitive to mean shifts, and the J-EWMA-Residual chart is sensitive to both mean and variance shifts. Implementation of the proposed chart to real data from an ingot growth process also shows that the AEWMA chart can successfully detect failure in the process. The AEWMA chart is simple in form, while the J-EWMA-Residual chart performance well in different out-of-control modes. Therefore, we recommend these two charts to the practitioners.

The dynamics of the real process usually has complicated engineering background. If such domain knowledge is taken into consideration and incorporated in chart design, it is expected to further improve the charting performance, which deserves further research efforts.

References:

Albin, S. L., Kang, L., and Shea, G. (1997). "An X and EWMA chart for individual observations." *Journal of Quality Technology*, 29(1), 41-48.

Capizzi, G., and Masarotto, G. (2003). "An adaptive exponentially weighted moving average control chart." *Technometrics*, 45(3), 199-207.

Chang, T. C., and Gan, F. F. (2006). "Monitoring linearity of measurement gauges." *Journal of Statistical Computation and Simulation*, 76(10), 889-911.

Crowder, S. V. (1987). "A Simple Method for Studying Run–Length Distributions of Exponentially Weighted Moving Average Charts." *Technometrics*, 29(4), 401-407.

Gupta, S., Montgomery, D., and Woodall, W. (2006). "Performance evaluation of two methods for online monitoring of linear calibration profiles." *International Journal of Production Research*, 44(10), 1927-1942.

Healy, J. D. (1987). "A note on multivariate CUSUM procedures." *Technometrics*, 29(4), 409-412.

Jin, R., and Liu, K. (2012). "Multimode Variation Modeling and Process Monitoring for Serial-Parallel Multistage Manufacturing Processes." *IIE Transactions*, 45, 617-629.

Lucas, J. M., and Saccucci, M. S. (1990). "Exponentially weighted moving average control schemes: properties and enhancements." *Technometrics*, 32(1), 1-12.

Macgregor, J. F., and Harris, T. J. (1993). "The Exponentially Weighted Moving Variance." *Journal of Quality Technology*, 25(2), 106-118.

Mahmoud, M. A., and Woodall, W. H. (2004). "Phase I analysis of linear profiles with calibration applications." *Technometrics*, 46(4), 380-391.

Noorossana. (2004a). "Monitoring Process Performance Using Linear Profiles ".

Reynolds, M. R., and Stoumbos, Z. G. (2006). "Comparisons of some exponentially weighted moving average control charts for monitoring the process mean and variance." *Technometrics*, 48(4), 550-567.

Shewhart, W. A. (1926). "Quality control charts." *Bell System Technical Journal*, 5, 593-603.

Spitzlsperger, G., Schmidt, C., Ernst, G., Strasser, H., and Speil, M. (2005). "Fault detection for a via etch process using adaptive multivariate methods." *IEEE Transactions on Semiconductor Manufacturing*, 18(4), 528-533.

Tsung, F., and Tsui, K. L. (2003). "A mean-shift pattern study on integration of SPC and APC for process monitoring." *IIE Transactions*, 35(3), 231-242.

Wang, K., and Tsung, F. (2007). "Monitoring feedback-controlled processes using adaptive T2 schemes." *International Journal of Production Research*, 45(23), 5601-5619.

Wang, K., and Tsung, F. (2008). "An adaptive T^2 chart for Monitoring Dynamic Systems." *Journal of Quality Technology*, 40, 109-123.

Woodall, W. H. (2000). "Controversies and contradictions in statistical process control." *Journal of Quality Technology*, 32(4), 341-350.

Woodall, W. H. (2007). "Current research on profile monitoring." *Produção*, 17(3), 420-425.

Woodall, W. H., and Maragah. (1990). "Discussion -- Exponentially Weighted Moving Average Control Schemes: Properties and Enhancements." *TECHNOMETRICS* volume 32 (NO. 1), 17-18.

Woodall, W. H., Spitzner, D. J., Montgomery, D. C., and Gupta, S. (2004). "Using control charts to monitor process and product quality profiles." *Journal of Quality Technology*, 36(3), 309-320.

Yashchin, E. (1987). "Some aspects of the theory of statistical control schemes." *IBM Journal of Research and Development*, 31(2), 199-205.

Yu, G., Zou, C., and Wang, Z. (2012). "Outlier Detection in Functional Observations With Applications to Profile Monitoring." *Technometrics*, 54(3), 308-318.

Zhu, J., and Lin, D. K. J. (2009). "Monitoring the slopes of linear profiles." *Quality Engineering*, 22(1), 1-12.

Zou, C., Zhang, Y., and Wang, Z. (2006). "A control chart based on a change-point model for monitoring linear profiles." *IIE Transactions*, 38(12), 1093-1103.

Zou, C., Zhou, C., Wang, Z., and Tsung, F. (2007). "A self-starting control chart for linear profiles." *Journal of Quality Technology*, 39(4), 364-375.